

Learning Cross-domain Semantic-Visual Relation for Transductive Zero-Shot Learning

Jianyang Zhang, Fengmao Lv, *Member, IEEE*, Guowu Yang, *Member, IEEE*, Lei Feng, Yufeng Yu, Lixin Duan, *Member, IEEE*,

Abstract—Zero-Shot Learning (ZSL) aims to learn recognition models for recognizing new classes without labeled data. In this work, we propose a novel approach dubbed Transferrable Semantic-Visual Relation (TSVR) to facilitate the cross-category transfer in transductive ZSL. Our approach draws on an intriguing insight connecting two challenging problems, *i.e.* domain adaptation and zero-shot learning. Domain adaptation aims to transfer knowledge across two different domains (*i.e.*, source domain and target domain) that share the identical task/label space. For ZSL, the source and target domains have different tasks/label spaces. Hence, ZSL is usually considered as a more difficult transfer setting compared with domain adaptation. Although the existing ZSL approaches use semantic attributes of categories to bridge the source and target domains, their performances are far from satisfactory due to the large domain gap between different categories. In contrast, our method directly transforms ZSL into a domain adaptation task through redrawing ZSL as predicting the similarity/dissimilarity labels for the pairs of semantic attributes and visual features. For this redrawn domain adaptation problem, we propose to use a domain-specific batch normalization component to reduce the domain discrepancy of semantic-visual pairs. Experimental results over diverse ZSL benchmarks clearly demonstrate the superiority of our method.

Index Terms—zero-shot learning, transfer learning, domain adaptation.

I. INTRODUCTION

ALTHOUGH deep learning has achieved great advances in image recognition over the past years, the corresponding performance leaps heavily rely on collecting sufficient labeled data for each category to be recognized [1], [2]. Due to the exponential growth of image data and potential classes, it usually requires a huge amount of time and human labor to collect well-labeled training data for new classes. This severely prevents deep learning from generalizing its prediction ability to new classes. To tackle this issue, Zero-Shot Learning (ZSL), which is originally inspired by humans' ability to recognize new objects without seeing samples, has attracted increasing attentions recently [3], [4], [5].

This work was done when J. Zhang worked as a research assistant at Southwestern University of Finance and Economics, supervised by F. Lv. (*Corresponding author: Fengmao Lv.*)

J. Zhang and F. Lv are with Center of Statistical Research and School of Statistics, Southwestern University of Finance and Economics, Sichuan 610074, China (e-mail: fengmaolv@126.com).

G. Yang and L. Duan are with School of Computer Science and Engineering, University of Electronic Science and Technology of China, Sichuan 611731, China.

L. Feng is with School of Computer Science and Engineering, Nanyang Technological University, 639798, Singapore.

Y. Yu is with School of Economics and Statistics, Guangzhou University, Guangdong 510006, China.

ZSL aims to learn recognition models which transfer knowledge from seen (source) classes with labeled samples to recognize novel (target) classes without labeled samples [6]. The main idea towards ZSL is to bridge the source and target classes by an intermediate-level semantic representation, which can be defined by attributes [3], word2vec [7], or WordNet [8]. Semantic representations, assumed to be shared between the source and target classes, constitute the key factor for cross-category transfer. To this end, most existing ZSL methods project visual features into the semantic representations and recognize images from novel target categories by nearest neighbor search in the shared space [6], [9], [10]. However, the projection functions learned from the source domain would be biased when they are directly applied to target images [11]. This is usually called as domain shift or projection shift. Although the recent transductive ZSL methods propose to leverage unlabeled images from novel classes to relieve the domain shift [12], [13], [14], the adaptation of projection function mainly relies on an iterative self-training procedure, in which the pseudo labels of target images are determined by directly leveraging semantic representations. Unfortunately, the potential relations between the source and target data are not explicitly aligned. Hence, the source and target categories are not sufficiently associated for transfer.

In this work, we propose a novel approach dubbed Transferrable Semantic-Visual Relation (TSVR) by drawing an intriguing insight connecting two challenging problems, which are domain adaptation and zero-shot learning, respectively. To be specific, domain adaptation aims at transferring knowledge across two different domains (*i.e.*, source domain and target domain) that share the identical task/label space [15]. However, for ZSL, the source and target domains have different tasks/label spaces. Therefore, the ZSL setting brings more challenges than domain adaptation. Motivated by this observation, we wonder whether it is beneficial if we directly transform transductive ZSL into an unsupervised domain adaptation problem through redrawing ZSL as predicting the similarity/dissimilarity labels for the pairs of semantic attributes and visual features. For this redrawn domain adaptation problem, the source domain contains semantic-visual pairs with similarity/dissimilarity labels and the target domain contains unlabeled semantic-visual pairs. The similarity labels of each pair can be predicted by a multi-layer metric network shared by both the two domains. In the existing domain adaptation approaches [16], [17], [18], the two domains can be bridged together through reducing the domain discrepancy of semantic-visual pairs.

In general, domain adversarial training is the most commonly used approach towards reducing the domain discrepancy in unsupervised domain adaptation [16], [19]. However, for the redrawn domain adaptation problem to be tackled in this work, the class distribution is extremely imbalanced, *i.e.* the number of the similar pairs is significantly smaller than that of the dissimilar ones. As a result, distribution alignment would be dominated by the large class in each mini-batch. Hence, domain adversarial training cannot be the best choice for our task. In this work, we propose to use a mild but effective component dubbed Domain-Specific Batch Normalization (DSBN) to align the distribution of semantic-visual pairs. Specifically, we incorporate two Batch Normalization (BN) units at each layer. This design enables the metric network to separately normalize the mini-batches from different domains with *zero* mean and *one* variance. Hence, the semantic-visual pairs from the source and target domains can have similar distribution at each layer of the metric network. Although the number of similar pairs is very small in each mini-batch, the moving average mechanism of batch normalization enables to retain their effect in feature alignment. Our approach is similar to Adaptive Batch Normalization (ABN) proposed from [18]. However, ABN only maintains the normalization statistics of source data at training and requires a separate process to modulate the normalization statistics for the target domain. Note that the target data cannot be used for training the network in ABN since they will cause bias in calculating the statistics of the source domain. In contrast, our design allows us to train the network by the target data through incorporating extra practical regularization terms over the target samples.

Overall, the main contribution of this work is two-fold. One is that we propose to tackle transductive ZSL as the domain adaptation problem which is a relatively easier task, through redrawing ZSL as predicting similarity/dissimilarity for the pair of visual images and categories' semantic attributes. The other is that, for this redrawn domain adaptation problem, we propose to use a domain-specific batch normalization component to align the distribution of semantic-visual pairs. Compared with the previous transductive ZSL methods that directly leverage the semantic representation to adapt the projection function [12], [13], [14], our proposal enables to more sufficiently exploit the potential relations between the source and target categories through aligning the distributions of semantic-visual pairs at hierarchical layers. Experimental results over diverse ZSL benchmarks clearly demonstrate the superiority of our method compared with the existing *state-of-the-art* ZSL methods.

The rest of the paper is organized as follows. Section II reviews the related works about zero-shot learning and domain adaptation. Section III introduces the motivation of our proposal. Section IV presents our approach for transductive ZSL. Section V presents our experimental results. Finally, Section VI summarizes this paper.

II. RELATED WORK

A. Zero-shot learning

Zero-Shot Learning aims to learn recognition models for recognizing new classes without labeled data. The main strat-

egy for ZSL is to associate source and target classes through an intermediate-level semantic representation. The semantic space can be defined by attributes [3], text description [20], word2vec [7], or WordNet [8]. In general, most existing ZSL methods project visual features into the semantic space and recognize images from novel target categories by nearest neighbor search in the shared space [6], [9], [10]. Unfortunately, nearest neighbor search in semantic space will suffer from the problem of hubness surfaces [21], [22]. To tackle this limitation, the recent works proposed to project semantic attributes into visual space as prototypes [23], [22], [24], [25]. In addition, the visual feature and the semantic representations can also be associated by projecting them into a shared intermediate space [26], [27]. However, the projection function learned from the source domain tends to be biased when they are directly applied to target images, which is usually named as domain shift or projection shift [11].

B. Transductive zero-shot learning

Transductive zero-shot learning aims to relieve the projection shift between the source and target categories through introducing unlabeled images from novel classes during training [11]. To be specific, Kodirov *et al.* [13] proposed to adapt the projection function by regularized sparse coding. Guo *et al.* [12] proposed a joint learning approach considering both source and target classes simultaneously to learn the shared model space. Ye *et al.* [14] proposed to simultaneously learn discriminative semantic representations for images from both the source and target classes, in order to prevent the potential projection shift problem. Later, Fu *et al.* [11] proposed a multi-view semantic space alignment process to alleviate the projection shift with multiple semantic views. More recently, Li *et al.* [28] proposed to leverage the target images with high confidence as the references to recognize other target data.

C. Domain adaptation

Domain adaptation aims at transferring knowledge across two different domains that share the identical task/label space. In general, the major challenge in domain adaptation lies in the distribution discrepancy between the source and the target domains. Therefore, the natural idea towards domain adaptation is to learn deep representations that can align the distributions of two domains. In general, the existing domain methods mainly relies on Mean Maximum Discrepancy (MMD) [17], [29] or domain adversarial training [16], [19] to reduce distribution discrepancy at intermediate layers of deep neural networks. In addition to the above methods, Li *et al.* [18] proposed that the statistics of BN layers is curtail for aligning distribution discrepancy. Compared with [18], our design enables to train the network with both the source and target data. Hence, we can incorporate extra practical regularization terms for the target data during the training phase.

III. MOTIVATION

Problem statement. Formally, the task of ZSL aims to learn recognition models for recognizing new classes without

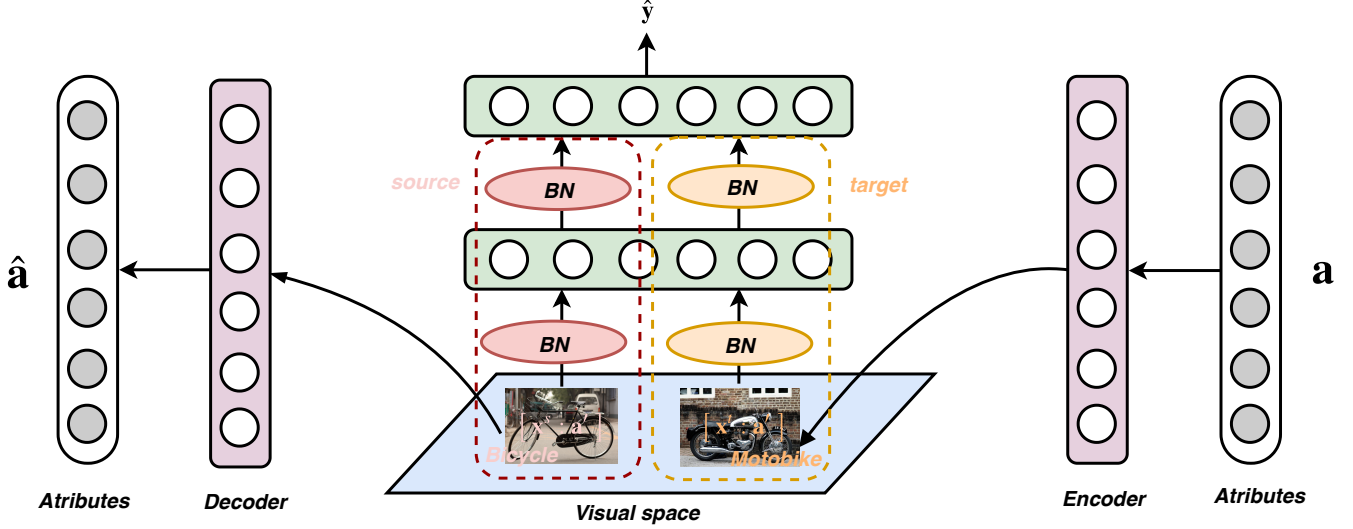


Fig. 1: The overall architecture of our proposed TSVR. The encoder transforms the semantic attributes \mathbf{a} into the visual space, with the transformed semantic attributes denoted by \mathbf{a}' . The multi-layer metric network takes the concatenated semantic-visual pairs $[\mathbf{x} : \mathbf{a}']$ as inputs and outputs their similarity score \hat{y} . The decoder takes the transformed semantic attributes \mathbf{a}' as input and outputs the reconstructed semantic attributes $\hat{\mathbf{a}}$. In each batch normalization layer, two BN units are used to normalize the mini-batches from the source and target domains separately.

labeled data. For the source domain, we are given a set of source categories $\mathcal{C}^s = \{c_1^s, \dots, c_{K_s}^s\}$ and a labeled dataset of source images $\mathcal{D}^s = \{(\mathbf{x}_1^s, \mathbf{y}_1^s), \dots, (\mathbf{x}_{N_s}^s, \mathbf{y}_{N_s}^s)\}$, where $\mathbf{x}_i^s \in \mathcal{R}^d$ is the image feature and $\mathbf{y}_i^s \in \{0, 1\}^{K_s}$ is the one-hot code indicating the class label of \mathbf{x}_i^s . In the transductive setting, we are also provided with an unlabeled target dataset $\mathcal{D}^t = \{\mathbf{x}_1^t, \dots, \mathbf{x}_{N_t}^t\}$. Note that the target images are from target categories $\mathcal{C}^t = \{c_1^t, \dots, c_{K_t}^t\}$ satisfying $\mathcal{C}^s \cap \mathcal{C}^t = \emptyset$. Albeit being disjoint, the source and target categories are assumed to share a common semantic space, on which each category $i \in \mathcal{C}^s \cup \mathcal{C}^t$ has a semantic representation $\mathbf{a}_i \in \mathcal{R}^r$. This shared space constitutes the key factor for cross-category transfer. To sum up, our goal is, given the labeled source data \mathcal{D}^s , the unlabeled target data \mathcal{D}^t and the semantic embeddings $\{\mathbf{a}_i\}_{i \in \mathcal{C}^s \cup \mathcal{C}^t}$ for training, to learn a prediction model which can the predict the label of target images from \mathcal{C}^t .

Zero-shot learning vs. domain adaptation. Transductive ZSL is for relieving the projection shift between the source and target categories through introducing unlabeled images from novel classes during training. Although the previous works claim to tackle the projection shift through domain adaptation [12], [13], their “domain adaptation” term actually means performing self-training for the target data through directly leveraging the semantic representation. Hence, the potential relations between the source and target data are not sufficiently explored for transfer. Using the approach from [12] as an example, we find that the source and target data are mainly associated by the direct relations of semantic attributes of each category, regardless of how to further reduce the domain discrepancy. As the source and target domains are defined by different label space, it is intractable to align the distributions using conventional domain adaptation approaches [17], [29]. Inspired by this observation, we wonder whether it is beneficial

if we transform transductive ZSL into a standard domain adaptation problem through redrawing ZSL as predicting the similarity/dissimilarity labels for the pairs of semantic attributes and visual features. The redrawn domain adaptation problem can be naturally tackled by using a multi-layer metric network to predict the similarity score of each semantic-visual pair. Then, the source and target domains can be aligned through reducing the domain discrepancy of semantic-visual pairs at intermediate layers of the metric network. The source and target domains can be more closely associated by aligning their distributions over multiple layers rather than merely utilizing the direct relation of semantic attributes.

Domain-specific batch normalization. To this end, the key point lies in how to reduce the distribution discrepancy of semantic-visual pairs from the source and target domains. In general, we can use MMD [17] or domain adversarial training [16] to align their distributions within each mini-batch. However, for this redrawn domain adaptation problem, it is worthy noting that the training data is extremely unbalanced, *i.e.* the number of negative pairs is significantly larger than that of positive pairs. For example, if the prediction task involves K categories, the number of the negative samples will be $K - 1$ times as large as that of the positive samples. Hence, there can be very few positive samples in each mini-batch. As a result, distribution alignment will be dominated by the large category if it is conducted over mini-batches. Motivated by this observation, we propose to align the distributions based on the batch normalization mechanism. To be specific, we incorporate two batch normalization units at each layer, which enables to separately normalize the mini-batches from different domains with *zero* mean and *one* variance. As a result, the distribution of semantic-visual pairs from both the source and target domains can be close to the standard normal distribution

over the intermediate layers of the metric network. Although the number of similar pairs is very small in each mini-batch, the moving average mechanism of batch normalization enables to retain their effect in feature alignment.

IV. TRANSFERRABLE SEMANTIC-VISUAL RELATION

The architecture of TSVR is shown in Fig. 1. Overall, we project the semantic representation into the visual space and leverage a hierarchical metric network shared by both two domains to predict the relation score of each semantic-visual pair. To align the distributions of semantic-visual pairs from the source and target domains, we incorporate two BN modules at each layer to maintain different normalization statistics for two domains during the training phase. Additionally, we incorporate an entropy minimization term as reasonable regularization for the unlabeled semantic-visual pairs from target domain.

A. From ZSL to domain adaptation

Problem transformation. The key idea of TSVR lies in tackling transductive ZSL as a domain adaptation task. To be specific, we adopt the pair of visual features and semantic attributes $(\mathbf{x}_i^s, \mathbf{a}_j^s)$, where $i = 1, \dots, N_s$ and $j = 1, \dots, K_s$, to redefine the training samples. Naturally, \mathbf{y}_{ij}^s is the label of $(\mathbf{x}_i^s, \mathbf{a}_j^s)$, indicating the similarity/dissimilarity of the corresponding semantic-visual pair. The target domain contains unlabeled semantic-visual pairs $(\mathbf{x}_i^t, \mathbf{a}_j^t)$, where $i = 1, \dots, N_t$ and $j = 1, \dots, K_t$. By this redefinition, the source and target domains will share the identical task, which leads to a standard unsupervised domain adaptation problem.

Theoretical insight. Our proposal also has a strong theoretical interpretation. The previous ZSL approaches usually use the compatibility function f to measure the relationship between visual features and semantic attributes. In general, f usually takes the following bilinear form:

$$f(\mathbf{x}, \mathbf{a}; \mathbf{W}) = \mathbf{x}^T \mathbf{W} \mathbf{a}, \quad (1)$$

where $\mathbf{W} \in \mathcal{R}^{d \times r}$. It is easy to verify that f can be equivalently formulated as follows:

$$f(\mathbf{x}, \mathbf{a}; \mathbf{u}) = (\mathbf{x} \otimes \mathbf{a})^T \mathbf{u}, \quad (2)$$

where $\mathbf{u} \in \mathcal{R}^{dr}$. Naturally, we can view $\mathbf{x} \otimes \mathbf{a}$ as a data instance. As a result, our problem can be treated as predicting the binary labels y_{ij} for the tensor product of visual features \mathbf{x}_i and semantic attributes \mathbf{a}_j . The binary label $y_{ij} \in \{0, 1\}$ indicates whether \mathbf{x}_i belongs to the j -th category. Hence, the loss function can be formulated as follows:

$$\min_{\mathbf{u}} \sum_{\mathbf{x}_i \in \mathcal{D}^s \cup \mathcal{D}^t} \sum_{j \in \mathcal{C}^s \cup \mathcal{C}^t} \ell(f(\mathbf{x}_i, \mathbf{a}_j; \mathbf{u}), y_{ij}). \quad (3)$$

With the target domain unlabeled, transductive ZSL aims to generalize the prediction ability of $f(\mathbf{x}, \mathbf{a}; \mathbf{u})$ trained with the labeled source domain to the target domain. Denote by $\hat{\mathcal{D}}^s = \{\mathbf{x}_i \otimes \mathbf{a}_j | \mathbf{x}_i \in \mathcal{D}^s, j \in \mathcal{C}^s\}$ and $\hat{\mathcal{D}}^t = \{\mathbf{x}_i \otimes \mathbf{a}_j | \mathbf{x}_i \in \mathcal{D}^t, j \in \mathcal{C}^t\}$ the set of semantic-visual pairs from the source and target domains, respectively. We can see that the distribution discrepancy between $\hat{\mathcal{D}}^s$ and $\hat{\mathcal{D}}^t$ establishes the bottleneck for

knowledge transfer in transductive ZSL, which is also the key point in the standard unsupervised domain adaptation problems. Denote by $\epsilon_s(f)$ and $\epsilon_t(f)$ the expected error of $f(\cdot; \mathbf{u})$ on the source and target semantic-visual pairs, respectively. Denote by $\hat{\mathcal{S}}$ and $\hat{\mathcal{T}}$ the underlying distributions of $\hat{\mathcal{D}}^s$ and $\hat{\mathcal{D}}^t$, respectively. From [30], $\epsilon_t(f)$ can be bounded as follows:

$$\epsilon_t(f) \leq \epsilon_s(f) + \frac{1}{2} d_{\mathcal{H}}(\hat{\mathcal{S}}, \hat{\mathcal{T}}) + \lambda, \forall f \in \mathcal{H}, \quad (4)$$

where

$$d_{\mathcal{H}}(\mathcal{S}, \mathcal{T}) = 2 \sup_{f \in \mathcal{H}} \left| \mathbf{Pr}_{\mathbf{x} \in \hat{\mathcal{S}}} [f(\mathbf{x}) = 1] - \mathbf{Pr}_{\mathbf{x} \in \hat{\mathcal{T}}} [f(\mathbf{x}) = 1] \right|, \quad (5)$$

$$\lambda = \min_{f \in \mathcal{H}} [\epsilon_s(f) + \epsilon_t(f)].$$

Hence, it is clear that reducing the distribution discrepancy of semantic-visual pairs can improve the performance of transductive ZSL.

Base model. We use a hierarchical metric network as the base model for the transformed domain adaptation problem. Since the dimension of the tensor product $\mathbf{x} \otimes \mathbf{a}$ can be very high, we concatenate the visual features and semantic attributes directly to construct the semantic-visual pairs. Moreover, to increase the flexibility, we use an encoder to transform the semantic attributes \mathbf{a} into the visual space. Denote by $\mathbf{a}' \in \mathcal{R}^{r'}$ and $[\mathbf{x} : \mathbf{a}'] \in \mathcal{R}^{d+r'}$ the transformed semantic attributes and the concatenated semantic-visual pairs, respectively. We then use a hierarchical metric network shared by both two domains to predict the relation score of each concatenated semantic-visual pair. The overall architecture of our model is clearly displayed in Fig. 1. It is worthy noting that this baseline has two advantages: 1) we can avoid the problem of hubness [21], [22], by considering visual space, instead of semantic space, as the embedding space; 2) we can more accurately capture the relation score of each semantic-visual pair by using a hierarchical metric network, instead of directly measuring their distance over the embedding space. Following [9], we incorporate a decoder for reconstructing the original semantic attributes, in order to enforce the transformed semantic attributes \mathbf{a}' to preserve their original semantic information. The reconstruction module is implemented by the L2 norm:

$$d_i = \|\mathbf{a}_i - \hat{\mathbf{a}}_i\|^2, \quad (6)$$

where $\hat{\mathbf{a}}_i$ is the output of the decoder.

There may exist a potential problem, *i.e.*, how to build mini-batches for training since the semantic-visual pairs are extremely imbalanced. For the source domain, we randomly select a fixed-size batch of images from \mathcal{D}^s , and then use categories existing in the current mini-batch to construct semantic-visual pairs for training. For the target domain, we will also select a mini-batch of images from \mathcal{D}^s , but all the categories from \mathcal{C}^t will be used to construct semantic-visual pairs since the target images do not have class labels.

B. Domain alignment

This work reduces the distribution discrepancy based on the recent advances of batch normalization. In this part, we first introduce the background of batch normalization. Then

we present how to utilize batch normalization for distribution alignment.

Preliminary: batch normalization. Batch normalization aims to keep the distribution of mini-batches unchanged across the intermediate layers of deep models. In this way, the training algorithm of deep neural networks can obtain more stable gradients to update the network parameters [31]. To be specific, BN normalizes the mini-batches with *zero* mean and *one* variance at each layer of deep neural networks. In each BN layer, we firstly calculate the mean and variance values of mini batches:

$$\begin{aligned}\mu^k &= \frac{1}{m} \sum_{i=1}^m x_i^k, \\ (\sigma^2)^k &= \frac{1}{m} \sum_{i=1}^m (x_i^k - \mu^k)^2,\end{aligned}\quad (7)$$

where x_i^k is the k -th element of the intermediate activation of the i -th sample in the current mini batch and m is the batch size. Then we normalize the intermediate activation to have *zero* mean and *one* variance:

$$\hat{x}^k = \frac{x^k - \mu^k}{\sqrt{(\sigma^2)^k + \epsilon}}, \quad (8)$$

where ϵ is a small value to avoid the problem of underflow. Moreover, in order to guarantee the flexibility of each intermediate layer, learnable scale and shift parameters, γ^k and β^k , are further used to transform the normalized activation \hat{x}^k :

$$z^k = \gamma^k \hat{x}^k + \beta^k. \quad (9)$$

Note that each BN layer will retain a set of global normalization statistics $\{\mu_g^k, \sigma_g^k\}$ using the moving average mechanism:

$$\begin{aligned}\mu_g^k &= \alpha \mu_g^k + (1 - \alpha) \mu^k, \\ \sigma_g^k &= \alpha \sigma_g^k + (1 - \alpha) \sigma^k,\end{aligned}\quad (10)$$

where μ^k and σ^k are the sample mean and sample standard deviation of the current mini-batch. In the testing phase, the BN layers use the global normalization statistics to normalize the testing data.

Domain-specific batch normalization. Although the standard batch normalization enables the deep model to obtain similar data distribution across different layers, it cannot lead to similar data distribution across different domains. In order to make the source and target data have similar distribution, we propose to incorporate two batch normalization units at each BN layer. This design enables deep models to separately normalize the mini-batches of different domains with *zero* mean and *one* variance.

Specifically, each BN layer will firstly calculate the mean and variance values for mini-batches of the source and target

Algorithm 1: Domain-specific batch normalization

Input: Dimension of intermediate layer K ; batch size m ; mini-batch of intermediate vectors $\{\mathbf{x}_i^s\}_{i=1}^m$ and $\{\mathbf{x}_i^t\}_{i=1}^m$, where $\mathbf{x}_i^s, \mathbf{x}_i^t \in \mathcal{R}^K$; scale and shift parameters: $\gamma, \beta \in \mathcal{R}^K$.

Output: normalized intermediate vectors $\{\mathbf{z}_i^s\}_{i=1}^m$ and $\{\mathbf{z}_i^t\}_{i=1}^m$, where $\mathbf{x}_i^s, \mathbf{x}_i^t \in \mathcal{R}^K$.

- 1 Calculate the mean values of each element:
 $\mu^{t(k)} = \frac{1}{m} \sum_{i=1}^m x_i^{t(k)}, \mu^{s(k)} = \frac{1}{m} \sum_{i=1}^m x_i^{s(k)}.$
 - 2 Calculate the variance values of each element:
 $(\sigma^2)^{s(k)} = \frac{1}{m} \sum_{i=1}^m (x_i^{s(k)} - \mu^{s(k)})^2, (\sigma^2)^{t(k)} = \frac{1}{m} \sum_{i=1}^m (x_i^{t(k)} - \mu^{t(k)})^2.$
 - 3 Normalize \mathbf{x}^s and \mathbf{x}^t separately:
 $\hat{x}^{s(k)} = \frac{x^{s(k)} - \mu^{s(k)}}{\sqrt{(\sigma^2)^{s(k)} + \epsilon}}, \hat{x}^{t(k)} = \frac{x^{t(k)} - \mu^{t(k)}}{\sqrt{(\sigma^2)^{t(k)} + \epsilon}}.$
 - 4 Transform the normalized vector by the scale and shift parameters: $z^{s(k)} = \gamma^k \hat{x}^{s(k)} + \beta^k, z^{t(k)} = \gamma^k \hat{x}^{t(k)} + \beta^k.$
-

domains separately:

$$\begin{aligned}\mu^{s(k)} &= \frac{1}{m} \sum_{i=1}^m x_i^{s(k)}, \mu^{t(k)} = \frac{1}{m} \sum_{i=1}^m x_i^{t(k)}, \\ (\sigma^2)^{s(k)} &= \frac{1}{m} \sum_{i=1}^m (x_i^{s(k)} - \mu^{s(k)})^2, \\ (\sigma^2)^{t(k)} &= \frac{1}{m} \sum_{i=1}^m (x_i^{t(k)} - \mu^{t(k)})^2.\end{aligned}\quad (11)$$

As a result, the source and target data can be normalized by their domain-specific normalization statistics:

$$\begin{aligned}\hat{x}^{s(k)} &= \frac{x^{s(k)} - \mu^{s(k)}}{\sqrt{(\sigma^2)^{s(k)} + \epsilon}}, \\ \hat{x}^{t(k)} &= \frac{x^{t(k)} - \mu^{t(k)}}{\sqrt{(\sigma^2)^{t(k)} + \epsilon}}.\end{aligned}\quad (12)$$

After that, the source and target data are transformed by the identical scale and shift parameters:

$$\begin{aligned}z^{s(k)} &= \gamma^k \hat{x}^{s(k)} + \beta^k, \\ z^{t(k)} &= \gamma^k \hat{x}^{t(k)} + \beta^k.\end{aligned}\quad (13)$$

The detailed calculating process within the domain-specific BN layer is shown in Algorithm 1. Note that each BN layer will also retain two sets of global normalization statistics, *i.e.* $\{\mu_g^{s(k)}, \sigma_g^{s(k)}\}$ and $\{\mu_g^{t(k)}, \sigma_g^{t(k)}\}$, to normalize the source and target testing data separately for final prediction.

The domain-specific batch normalization approach suits our redefined domain adaptation problem well. Although the number of positive pairs is very small in each mini-batch, the moving average mechanism of batch normalization enables to retain their effect in feature alignment. Compared to MMD or domain adversarial training which align distributions over mini-batches, the problem of data imbalance can be alleviated. Moreover, our design is very easy-to-implement, without introducing extra hyper-parameters or mini-max problems which

are often difficult to be optimized. Compared with [18], the domain-specific batch normalization design allows us to train the network by the target data, without introducing bias in the normalization statistics.

Theoretical insight. From Eq. 4, it is clear that the distribution discrepancy between $\hat{\mathcal{S}}$ and $\hat{\mathcal{T}}$ builds the main bottleneck for knowledge transfer in domain adaptation. In Theorem 1, we show the theoretical interpretation of domain-specific batch normalization.

Theorem 1: Domain-specific batch normalization is trying to reduce the upper bound $d_{\mathcal{H}}(\hat{\mathcal{S}}, \hat{\mathcal{T}})$.

Proof: It is clear that $d_{\mathcal{H}}(\hat{\mathcal{S}}, \hat{\mathcal{T}})$ satisfies the triangular inequation:

$$\begin{aligned} d_{\mathcal{H}}(\mathcal{S}, \mathcal{T}) &= 2 \sup_{f \in \mathcal{H}} \left| \Pr_{\mathbf{x} \in \hat{\mathcal{S}}} [f(\mathbf{x}) = 1] - \Pr_{\mathbf{x} \in \hat{\mathcal{T}}} [f(\mathbf{x}) = 1] \right| \\ &\leq 2 \sup_{f \in \mathcal{H}} \left| \Pr_{\mathbf{x} \in \hat{\mathcal{S}}} [f(\mathbf{x}) = 1] - \Pr_{\mathbf{x} \in \mathcal{P}} (\mathbf{x}) \right| + \\ &\quad 2 \sup_{f \in \mathcal{H}} \left| \Pr_{\mathbf{x} \in \hat{\mathcal{T}}} [f(\mathbf{x}) = 1] - \Pr_{\mathbf{x} \in \mathcal{P}} (\mathbf{x}) \right| \\ &= d_{\mathcal{H}}(\hat{\mathcal{S}}, \mathcal{P}) + d_{\mathcal{H}}(\hat{\mathcal{T}}, \mathcal{P}). \end{aligned} \quad (14)$$

The distribution \mathcal{P} satisfies the condition that $\mathcal{P}_k \sim \mathcal{N}(0, 1)$, where \mathcal{P}_k is the marginal distribution of \mathcal{P} at each dimension. Denote by $\hat{\mathcal{S}}_k$ and $\hat{\mathcal{T}}_k$ the marginal distributions of each dimension of the source and target domains, respectively. In each domain, the domain-specific batch normalization unit enforces the marginal distribution of each dimension of the data instance to approximate the normal distribution: $\hat{\mathcal{S}}_k \rightarrow \mathcal{N}(0, 1)$ and $\hat{\mathcal{T}}_k \rightarrow \mathcal{N}(0, 1)$. As a result, the last two terms of Eq. 14 will be enforced to be close to 0. Hence, domain-specific batch normalization gives a tighter upper bound for the expected error $\epsilon_t(f)$. ■

C. Practical entropy regularization

Furthermore, we also incorporate practical regularization for the prediction of unlabeled semantic-visual pairs from the target domain. We regularize the metric network by leveraging the property that a target image can only relate to one category from \mathcal{C}^t . Through enforcing the metric network to reach this property, we can strengthen the network's generalization ability to the target domain. To implement this, we design an entropy minimization loss for the target semantic-visual pairs. To be specific, for a target image \mathbf{x}_i^t , we collect the metric network's outputs of each semantic-visual pair as a vector: $\mathbf{Z}_i^t = [\mathbf{z}_{i1}^t, \dots, \mathbf{z}_{iK_t}^t]$, where \mathbf{z}_{ij}^t is the output for the pair of \mathbf{x}_i^t and \mathbf{a}_j^t . Note that \mathbf{z}_{ij}^t is collected before the sigmoid layer for avoiding the problem of gradient vanishing. Then we use a softmax operation to process \mathbf{Z}_i^t , resulting in a probability vector $\mathbf{P}_i^t = [\mathbf{p}_{i1}^t, \dots, \mathbf{p}_{iK_t}^t]$ that describes which category the target image \mathbf{x}_i^t belongs. To utilize the target property as indicated above, we propose to minimize the entropy of that probability vector since small entropy implies low-density separation between categories [32]. Formally, the entropy of is defined as:

$$H(\mathbf{P}_i^t) = - \sum_{j=1}^{K_t} \mathbf{p}_{ij}^t \log \mathbf{p}_{ij}^t. \quad (15)$$

D. Training

From our definition of the redrawn domain adaptation problem, only the source semantic-visual pairs have similarity/dissimilarity labels. Hence, using $\hat{\mathbf{y}}_{ij}^s$ to denote the metric network's prediction for the pair of \mathbf{x}_i^s and \mathbf{a}_j^s , we can train the metric network via a cross-entropy loss in the source domain:

$$\mathcal{L}_{\text{pre}} = - \frac{1}{N_s} \frac{1}{K_s} \sum_{i=1}^{N_t} \sum_{j=1}^{K_s} \left[(\mathbf{y}_{ij}^s - 1) \log \frac{\hat{\mathbf{y}}_{ij}^s}{1 + \hat{\mathbf{y}}_{ij}^s} - \mathbf{y}_{ij}^s \log \frac{1}{1 + \hat{\mathbf{y}}_{ij}^s} \right]. \quad (16)$$

The entropy regularization loss defined for target semantic-visual pairs is formalized as:

$$\mathcal{L}_{\text{ent}} = \frac{1}{N_t} \sum_{i=1}^{N_t} H(\mathbf{P}_i^t). \quad (17)$$

The reconstruction loss is computed for the semantic attributes of both source and target categories:

$$\mathcal{L}_{\text{rec}} = \frac{1}{K_s} \sum_{i=1}^{K_s} d_i^s + \frac{1}{K_t} \sum_{i=1}^{K_t} d_i^t. \quad (18)$$

In conclusion, with the above sub-objectives, our final objective function is formulated as follows:

$$\min \mathcal{L}_{\text{pre}} + \lambda_{\text{ent}} \mathcal{L}_{\text{ent}} + \lambda_{\text{rec}} \mathcal{L}_{\text{rec}}, \quad (19)$$

where λ_{rec} and λ_{ent} are hyper-parameters that weigh the importance of the corresponding terms. It is worthy noting that our design for domain alignment does not introduce any loss terms, as well as extra hyper-parameters. In optimization, the encoder for semantic attributes receives gradients from all the three loss terms, while the metric network receives gradients from the first two terms.

E. Prediction

After the training phase is finished, we can obtain the metric network's prediction $\hat{\mathbf{y}}_{ij}^t$ for target semantic-visual pairs. Specifically, $\hat{\mathbf{y}}_{ij}^t$ reveals the relation score of the pair of image \mathbf{x}_i^t and attribute \mathbf{a}_j^t . Hence, we can predict the label of target image \mathbf{x}_i^t as the class with the largest relation score:

$$k^* = \operatorname{argmax}_{j \in \mathcal{C}^t} \hat{\mathbf{y}}_{ij}^t. \quad (20)$$

V. EXPERIMENTS

A. Datasets

We conduct experiments on four standard ZSL datasets: 1) attribute-Pascal-Yahoo (aPY) [33]; 2) Animal with Attribute (AwA) [34]; 3) Caltech-UCSD Birds 200-2011 (CUB) [35]; 4) SUN-Attribute (SUN) [36]. The aPY dataset has 12,695 images of 20 classes from Pascal and 2,644 images of 12 classes from Yahoo. The images of aPY are labeled by 64 dim binary vectors for denoting the semantic attributes. For aPY, the source domain includes 20 categories and the target domain has 12 ones. AwA contains 37,322 images from 50 categories. For AwA, the source and target domains have 40 and 10 categories, respectively. The images in AwA are labeled by 85-dimensional semantic attributes. The CUB dataset contains 11,788 images over 200 bird species, in which 150 species are used as the source categories and the rest 50 as the target. The

images in CUB are labeled by 312 dimensional continuous vectors. The SUN dataset contains 14,140 images over 717 categories, with each image labeled by a 102 dimensional attribute vector. For SUN, the source and target domains contain 645 and 72 categories, respectively.

B. Implementation details

Our method is implemented by the PyTorch framework. In all the experiments, the image embeddings are 2048 dimensional features obtained from the top-layer units of ResNet-101. The ResNet-101 is pre-trained on ImageNet with 1K classes. Both the encoder and decoder networks include one hidden layer with 1250 units. The metric network contains two fully connected layers with 1250 hidden units. In our experiments, Adam is utilized as the optimizer. We set the initial learning rate to 10^{-5} . The maximum iteration number is 50,000 and the batch size is set to 32. The trade-off parameters λ_{rec} and λ_{ent} are set to 10^{-5} and 10^{-9} , respectively. Our experimental results are insensitive to their values. Like the existing *state-of-the-art* transductive ZSL methods [13], [14], [34], we adopt the label propagation step to refine the final prediction results.

In our experiments, we employ both the standard splits (SS) and the proposed splits (PS) from [34] for fair comparisons. We use the Mean Class Accuracy (MCA) as our evaluation metric, which is defined as follows:

$$\text{MCA} = \frac{1}{|\mathcal{C}^t|} \sum_{y \in \mathcal{C}^t} \text{acc}_y, \quad (21)$$

where acc_y denotes the prediction accuracy over the test data of class y . The experimental results are averaged over five independent trails. Note that we do not conduct experiments for the generalized setting since it is ill-posed for transductive ZSL: 1) The transductive setting means that the unlabeled data of the training phase will also be the data for testing, which is true for ZSL as well [34]. Actually, this is problematic for the generalized ZSL setting, since the model has already known that the unlabeled data are from the target categories during training. 2) Since both the source and target images are available for training, we can naively train a binary classifier for predicting the domain label of testing data. Hence, the performance will mainly rely on the capacity of the binary classifier.

C. Baselines

To demonstrate the effectiveness of TSVR, we conduct extensive comparison studies with diverse models, including both inductive ZSL and transductive ZSL baselines, which are clearly listed as follows.

Inductive ZSL baselines.

- **ALE**: Attribute Label Embedding from [6]. It projects visual features into the semantic space and uses a compatibility matrix to measure the distances.
- **SAE**: Semantic AutoEncoder from [9]. It uses the autoencoder framework to improve the generalization capacity to the target domain.

- **DCN**: Deep Calibration Network proposed in [37]. It calibrates the network based on the confidence of source classes and uncertainty of target classes.
- **SRN**: Semantic Relation Network from [5]. It proposes to utilize the structure of semantic attributes to induce semanticity to visual space.
- **SP-AEN**: Semantics-Preserving Adversarial Embedding Networks from [38]. It tackles the semantic loss problem in ZSL by introducing a novel visual reconstruction paradigm.
- **SE-ZSL**: Zero-Shot Learning via Synthesized Examples proposed in [39]. It designs a variational autoencoder based architecture to generate samples of the target categories.
- **f-CLSWGAN**: a novel GAN-method from [24]. It leverages generative adversarial networks to generate samples of the target categories.

Transductive ZSL baselines.

- **ALE-T**: Attribute Label Embedding for transductive ZSL, proposed in [40]. It leverages a label propagation procedure to refine the results of ALE.
- **UDA**: Unsupervised Domain Adaptation for zero-shot learning proposed in [13]. It proposes to adapt the projection function by regularized sparse coding.
- **SMSL**: Shared Model Space Learning proposed in [12]. It is a joint learning approach considering both source and target classes simultaneously to learn the shared model space.
- **TMVL**: Transductive Multi-View Learning from [11]. It proposes a multi-view semantic space alignment process to alleviate the projection shift with multiple semantic views.
- **LisGAN**: Leveraging invariant side Generative Adversarial Network proposed in [28]. It leverages the target images with high confidence as the reference to recognize other target data.

D. Performance Comparison

The experimental results of our method and the existing *state-of-the-art* ZSL methods are reported in Table I. For more convincing comparisons, we report the results of both the SS and PS settings. It is clearly that: 1) in general, the transductive baselines usually have better performance than the inductive baselines by introducing unlabeled data from the target categories for training; 2) our performance is on par with or better than the existing *state-of-the-art* baselines. Specifically, with label propagation as the only transductive design, ALE-T cannot sufficiently exploit the potential semantic relations between the source and target categories. Compared with UDA or SMSL, our model can more closely associate the source and target categories by aligning their distributions over multiple layers rather than merely utilizing the direct relation of semantic representation. For TMVL, although it exploits multiple intermediate semantic representations, its performance is still unsatisfactory. It is also worthy noting that our method is very easy-to-implement, without introducing tedious EM optimization procedures like SMSL. Compared

TABLE I: Comparisons with the existing *state-of-the-art* ZSL baselines in each setting. The notation \mathcal{I} denotes the inductive baselines and \mathcal{T} denotes the transductive baselines.

	Model	CUB		aPY		AwA		SUN	
		PS	SS	PS	SS	PS	SS	PS	SS
\mathcal{I}	ALE	54.9%	53.2%	39.7%	30.9%	62.5%	80.3%	58.1%	59.1%
	SAE	33.3%	33.4%	8.3%	8.3%	54.1%	80.7%	40.3%	42.4%
	DCN	56.2%	55.6%	43.6%	-	65.2%	82.3%	61.8%	67.4%
	SRN	56.0%	-	38.4%	-	-	-	61.4%	-
	SP-AEN	55.4%	-	24.1%	-	58.5%	-	59.2%	-
	SE-ZSL	59.6%	60.3%	-	-	69.5%	83.8%	63.4%	64.5%
	f-CLSWGAN	57.3%	-	-	-	68.2%	-	60.8%	-
\mathcal{T}	ALE-T	54.5%	59.4%	46.4%	-	70.6%	-	55.4%	-
	UDA	-	39.5%	-	-	-	-	-	-
	SMSL	-	-	-	39.0%	-	-	-	-
	TMVL	-	47.9%	-	-	-	-	-	-
	LisGAN	58.8%	-	43.1%	-	70.6%	-	61.7%	-
ours	TSVR	61.0%	60.9%	53.3%	46.3%	74.6%	93.2%	64.7%	66.7%

TABLE II: Ablation study for the contribution of each design over the PS setting. “Baseline” indicates the metric network trained with only the semantic-visual pairs from the source domain; “-2BN” indicates using only one batch normalization unit in each BN layer. “-reconstruct” and “-entropy” indicate removing \mathcal{L}_{rec} and \mathcal{L}_{ent} from the overall objective, respectively; “DANN” and “MMD” indicate replacing the distribution alignment approach with domain adversarial training and MMD, respectively.

	CUB	aPY	AwA	SUN
Baseline	58.0%	35.9%	62.4%	63.1%
Full model	61.0%	53.3%	74.6%	64.7%
-2BN	59.4%	49.4%	67.7%	64.1%
-reconstruct	59.5%	46.7%	65.0%	62.6%
-entropy	61.8%	49.1%	68.4%	64.1%
DANN	57.4%	49.8%	68.5%	63.5%
MMD	59.4%	49.4%	69.0%	62.9%

with LisGAN, our method does not need to solve the mini-max problems which are often difficult to optimize.

E. Analysis

As displayed in Table II, we further conduct the ablation study to demonstrate the contributions of each design in TSVR. The first row represents the metric network trained with only the semantic-visual pairs from source domain. From the next four rows, it is clear that all the key points designed in our approach generally make a good contribution to promoting knowledge transfer in ZSL. The performance improvement of \mathcal{L}_{ent} can be limited if the target domain involves two many categories, which is clearly revealed by “CUB” and “SUN”. From the last two rows, we can see that the performance is not good if domain adversarial training or MMD is used for

distribution alignment. This observation is consistent with our motivation.

Fig. 2 displays the t-SNE visualization for the metric network’s intermediate layers. We can see that there exists clear domain discrepancy between the distributions of the semantic-visual pairs from two domains. By using two BN modules to separately normalize the mini-batches from different domains, our design can effectively align the distribution discrepancy.

Finally, we conduct the sensitivity analysis for hyper-parameters to demonstrate the robustness of our model, which is clearly displayed in Fig. 3. In particular, we conduct experiments varying the trade-off parameters, including λ_{rec} for the attribute reconstruction loss and λ_{ent} for the entropy regularization loss. From Fig. 3, we can see that the performance of TSVR is not sensitive to the values of the trade-off parameters.

VI. CONCLUSION

In this paper, we propose a novel approach dubbed Transferable Semantic-Visual Relation for transductive ZSL. To be specific, we propose to transform transductive ZSL into an unsupervised domain adaptation problem through redrawing ZSL as predicting similarity score for the pairs of semantic attributes and visual features. Compared with transductive ZSL, domain adaptation is a relatively easier transfer setting since the source and target domains have the identical label space. To reduce the distribution discrepancy of semantic-visual pairs for the redrawn domain adaptation problem, we propose to incorporate two batch normalization units at each BN layer to normalize the mini-batches from the source and target domains separately. As a result, the source and target data can follow similar distribution at each layer of the metric network. Compared with the previous transductive ZSL methods that utilize the direct relation of semantic attributes for cross-category transfer, our method can more sufficiently explore the potential relations between the source and target categories

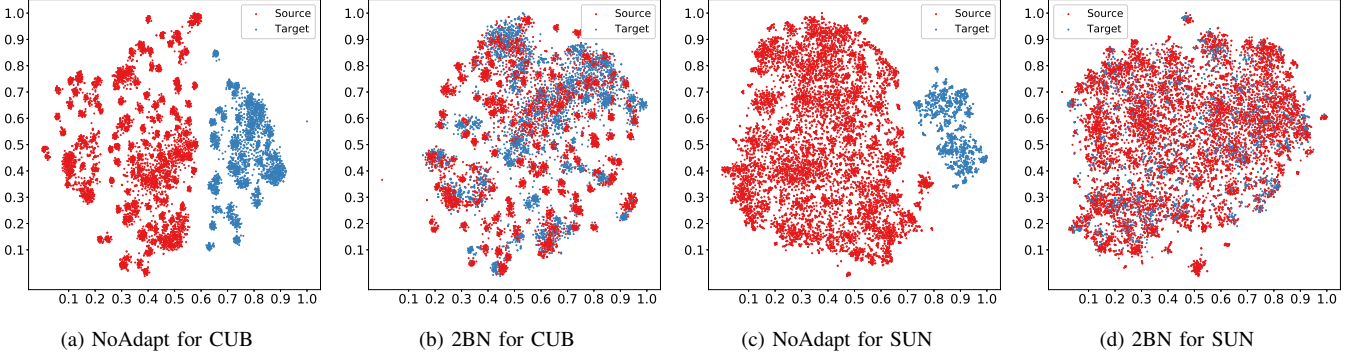


Fig. 2: The t-SNE visualization for intermediate layers of the metric network.

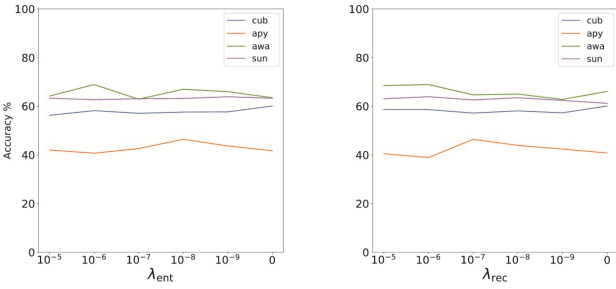


Fig. 3: Sensitivity analysis for the hyper-parameters.

through aligning the distributions of semantic-visual pairs over multiple layers. Experimental results over diverse ZSL benchmarks clearly demonstrate the superiority of our method compared with the existing *state-of-the-art* ZSL works.

ACKNOWLEDGEMENTS

This paper is supported by the National Natural Science Foundation of China (No. 11829101 and 11931014), and the Fundamental Research Funds for the Central Universities of China (No. JBK1806002). The authors would like to thank the anonymous reviewers for the careful reading of this paper and the constructive comments they provided.

REFERENCES

- [1] A. Krizhevsky, I. Sutskever, and G. E. Hinton, “Imagenet classification with deep convolutional neural networks,” in *Advances in neural information processing systems*, 2012, pp. 1097–1105.
- [2] K. He, X. Zhang, S. Ren, and J. Sun, “Deep residual learning for image recognition,” in *IEEE Conference on Computer Vision & Pattern Recognition*, 2016, pp. 770–778.
- [3] M. Palatucci, D. Pomerleau, G. E. Hinton, and T. M. Mitchell, “Zero-shot learning with semantic output codes,” in *Advances in neural information processing systems*, 2009, pp. 1410–1418.
- [4] Z. Zhang and V. Saligrama, “Zero-shot learning via semantic similarity embedding,” in *International Conference on Computer Vision*, 2015, pp. 4166–4174.
- [5] Y. Annadani and S. Biswas, “Preserving semantic relations for zero-shot learning,” in *IEEE Conference on Computer Vision & Pattern Recognition*, 2018, pp. 7603–7612.
- [6] Z. Akata, F. Perronnin, Z. Harchaoui, and C. Schmid, “Label-embedding for attribute-based classification,” in *IEEE Conference on Computer Vision & Pattern Recognition*, 2013, pp. 819–826.
- [7] T. Mikolov, K. Chen, G. Corrado, and J. Dean, “Efficient estimation of word representations in vector space,” *arXiv preprint arXiv:1301.3781*, 2013.
- [8] G. A. Miller, “Wordnet: a lexical database for english,” *ACM International Conference on Multimedia*, vol. 38, no. 11, pp. 39–41, 1995.
- [9] E. Kodirov, T. Xiang, and S. Gong, “Semantic autoencoder for zero-shot learning,” in *IEEE Conference on Computer Vision & Pattern Recognition*, 2017, pp. 3174–3183.
- [10] Z. Akata, S. Reed, D. Walter, H. Lee, and B. Schiele, “Evaluation of output embeddings for fine-grained image classification,” in *IEEE Conference on Computer Vision & Pattern Recognition*, 2015, pp. 2927–2936.
- [11] Y. Fu, T. M. Hospedales, T. Xiang, and S. Gong, “Transductive multi-view zero-shot learning,” *IEEE Transactions on Pattern Analysis & Machine Intelligence*, vol. 37, no. 11, pp. 2332–2345, 2015.
- [12] Y. Guo, G. Ding, X. Jin, and J. Wang, “Transductive zero-shot recognition via shared model space learning,” in *AAAI Conference on Artificial Intelligence*, 2016.
- [13] E. Kodirov, T. Xiang, Z. Fu, and S. Gong, “Unsupervised domain adaptation for zero-shot learning,” in *IEEE International Conference on Computer Vision*, 2015, pp. 2452–2460.
- [14] M. Ye and Y. Guo, “Zero-shot classification with discriminative semantic representation learning,” in *IEEE Conference on Computer Vision & Pattern Recognition*, 2017, pp. 7140–7148.
- [15] S. J. Pan and Q. Yang, “A survey on transfer learning,” *IEEE Transactions on Knowledge and Data Engineering*, vol. 22, no. 10, pp. 1345–1359, 2009.
- [16] Y. Ganin and V. Lempitsky, “Unsupervised domain adaptation by backpropagation,” *arXiv preprint arXiv:1409.7495*, 2014.
- [17] M. Long, Y. Cao, J. Wang, and M. I. Jordan, “Learning transferable features with deep adaptation networks,” *arXiv preprint arXiv:1502.02791*, 2015.
- [18] Y. Li, N. Wang, J. Shi, X. Hou, and J. Liu, “Adaptive batch normalization for practical domain adaptation,” *Pattern Recognition*, vol. 80, pp. 109–117, 2018.
- [19] E. Tzeng, J. Hoffman, K. Saenko, and T. Darrell, “Adversarial discriminative domain adaptation,” in *IEEE Conference on Computer Vision & Pattern Recognition*, 2017, pp. 7167–7176.
- [20] Y. Zhu, M. Elhoseiny, B. Liu, X. Peng, and A. Elgammal, “A generative adversarial approach for zero-shot learning from noisy texts,” in *IEEE Conference on Computer Vision & Pattern Recognition*, 2018, pp. 1004–1013.
- [21] M. Radovanović, A. Nanopoulos, and M. Ivanović, “Hubs in space: Popular nearest neighbors in high-dimensional data,” *Journal of Machine Learning Research*, vol. 11, no. Sep, pp. 2487–2531, 2010.
- [22] Y. Shigeto, I. Suzuki, K. Hara, M. Shimbo, and Y. Matsumoto, “Ridge regression, hubness, and zero-shot learning,” in *European Conference on Machine Learning*. Springer, 2015, pp. 135–151.
- [23] L. Zhang, T. Xiang, and S. Gong, “Learning a deep embedding model for zero-shot learning,” in *IEEE Conference on Computer Vision & Pattern Recognition*, 2017, pp. 2021–2030.
- [24] Y. Xian, T. Lorenz, B. Schiele, and Z. Akata, “Feature generating networks for zero-shot learning,” in *IEEE Conference on Computer Vision & Pattern Recognition*, 2018, pp. 5542–5551.
- [25] F. Sung, Y. Yang, L. Zhang, T. Xiang, P. H. Torr, and T. M. Hospedales, “Learning to compare: Relation network for few-shot learning,” in *IEEE*

- Conference on Computer Vision & Pattern Recognition*, 2018, pp. 1199–1208.
- [26] Z. Zhang and V. Saligrama, “Zero-shot learning via joint latent similarity embedding,” in *IEEE Conference on Computer Vision & Pattern Recognition*, 2016, pp. 6034–6042.
 - [27] H. Jiang, R. Wang, S. Shan, and X. Chen, “Learning class prototypes via structure alignment for zero-shot recognition,” in *European Conference on Computer Vision*, 2018, pp. 118–134.
 - [28] J. Li, M. Jin, K. Lu, Z. Ding, L. Zhu, and Z. Huang, “Leveraging the invariant side of generative zero-shot learning,” *arXiv preprint arXiv:1904.04092*, 2019.
 - [29] M. Long, H. Zhu, J. Wang, and M. I. Jordan, “Deep transfer learning with joint adaptation networks,” in *International Conference on Machine Learning*. JMLR. org, 2017, pp. 2208–2217.
 - [30] S. Ben-David, J. Blitzer, K. Crammer, A. Kulesza, F. Pereira, and J. Vaughan, “A theory of learning from different domains,” *Machine Learning*, vol. 79, pp. 151–175, 2010. [Online]. Available: <http://www.springerlink.com/content/q6qk230685577n52/>
 - [31] S. Ioffe and C. Szegedy, “Batch normalization: Accelerating deep network training by reducing internal covariate shift,” in *Proceedings of the 32nd International Conference on International Conference on Machine Learning - Volume 37*, ser. ICML15. JMLR.org, 2015, p. 448456.
 - [32] A. Krause, P. Perona, and R. G. Gomes, “Discriminative clustering by regularized information maximization,” in *Advances in neural information processing systems*, 2010, pp. 775–783.
 - [33] A. Farhadi, I. Endres, D. Hoiem, and D. Forsyth, “Describing objects by their attributes,” in *IEEE Conference on Computer Vision & Pattern Recognition*. IEEE, 2009, pp. 1778–1785.
 - [34] Y. Xian, C. H. Lampert, B. Schiele, and Z. Akata, “Zero-shot learning-a comprehensive evaluation of the good, the bad and the ugly,” *IEEE Transactions on Pattern Analysis & Machine Intelligence*, 2018.
 - [35] C. Wah, S. Branson, P. Welinder, P. Perona, and S. Belongie, “The caltech-ucsd birds-200-2011 dataset,” 2011.
 - [36] G. Patterson and J. Hays, “Sun attribute database: Discovering, annotating, and recognizing scene attributes,” in *IEEE Conference on Computer Vision & Pattern Recognition*. IEEE, 2012, pp. 2751–2758.
 - [37] S. Liu, M. Long, J. Wang, and M. I. Jordan, “Generalized zero-shot learning with deep calibration network,” in *Advances in neural information processing systems*, 2018, pp. 2005–2015.
 - [38] L. Chen, H. Zhang, J. Xiao, W. Liu, and S.-F. Chang, “Zero-shot visual recognition using semantics-preserving adversarial embedding networks,” in *IEEE Conference on Computer Vision & Pattern Recognition*, 2018, pp. 1043–1052.
 - [39] V. Kumar Verma, G. Arora, A. Mishra, and P. Rai, “Generalized zero-shot learning via synthesized examples,” in *IEEE Conference on Computer Vision & Pattern Recognition*, 2018, pp. 4281–4289.
 - [40] Z. Akata, F. Perronnin, Z. Harchaoui, and C. Schmid, “Label-embedding for image classification,” *IEEE Transactions on Pattern Analysis & Machine Intelligence*, vol. 38, no. 7, pp. 1425–1438, 2015.